

## Supporting Information

### Water Nanoconfined in Clays. The Structure of Na Vermiculite Revisited by Ab Initio Simulations

Pierfranco Demontis,<sup>†</sup> Marco Masia<sup>†§</sup> and Giuseppe B. Suffritti<sup>†\*</sup>

<sup>†</sup> *Dipartimento di Chimica e Farmacia, Università degli studi di Sassari and Consorzio Interuniversitario Nazionale per la Scienza e Tecnologia dei Materiali (INSTM), Unità di ricerca di Sassari, I- 07100 Sassari (Italy)*

<sup>§</sup> *Istituto Officina dei Materiali del CNR, UOS SLACS, Via Vienna 2, 07100 Sassari, Italy*

---

*\*) Corresponding author:*

Giuseppe B. Suffritti

Dipartimento di Chimica e Farmacia

Università degli studi di Sassari

Via Vienna, 2,

I-07100 Sassari

Italy

Phone: +39-079-229552

Fax: +39-079-229559

E-mail: pino@uniss.it

## Examples of previous *ab initio* studied of hydrated clays

We report here some meaningful examples of *ab initio* studies of hydrated clays. A review of the investigations performed until 2005 can be found in Reference S1. Tunega *et al.*<sup>S2</sup> performed *ab initio* molecular dynamics room-temperature simulations in the study of absorption sites on the octahedral and tetrahedral surface of the kaolinite group clay minerals,<sup>S3,S4</sup> belonging to the 1:1 layer type. Interactions water and acetic acid with both tetrahedral and octahedral surfaces were investigated. Both the localized density approximation (LDA) and the generalized gradient approximation (GGA) were used. The LDA was parametrized according to Perdew–Zunger<sup>S5</sup> and the GGA according to Perdew–Wang.<sup>S6</sup> The calculations were performed in a plane-wave basis set using the projector-augmented wave (PAW) method<sup>S7,S8</sup> and ultrasoft pseudo-potentials.<sup>S9,S10</sup> It was found that hydroxyl groups present on the octahedral surface form hydrogen bonds (HBs) with adsorbed molecules and that both molecules interact only very weakly with the tetrahedral side of the kaolinite layer showing the hydrophobicity of this surface.

Boek and Sprik<sup>S11</sup> studied the structure and the dynamics of smectite using a plane wave implementation of Kohn–Sham DFT. Smectites are a clay group belonging to the 2:1 layer type as vermiculite, but with a smaller layer charge (typically  $-0.5 e$ ).<sup>S3,S4</sup> The calculations were based on the BLYP energy functional, including the exchange contribution by Becke<sup>S10</sup> and a correlation term according to Lee–Yang–Parr.<sup>S12</sup> Kohn–Sham orbitals were expanded in plane waves in combination with medium-soft norm-conserving pseudopotentials according to the Troullier–Martins (TM) scheme.<sup>S13</sup> Both dehydrated and double-layer hydrated clays were considered, including one  $\text{Na}^+$  cation and 16 water molecules for the hydrated clay. The last system was similar to that considered in this work, the main difference consisting in a smaller sheet charge, thus entailing weaker HBs of water with the sheets and a liquid-like behavior of water itself. The  $\text{Na}^+$  cation remained around the plane at  $z/c = 0.500$ , but in a subsequent study,<sup>S14</sup> constrained dynamics was used to evaluate the free energy profile for the adsorption of  $\text{Na}^+$  cations on the smectite surface in the same system. It resulted that “there was a large preference for the  $\text{Na}^+$  to reside at  $z \approx 6.1 \text{ \AA}$  from the center of the clay layer, [where] the ion is bound to one surface O atom and the coordination of the ion is completed by four interlayer water molecules. [...] The midpoint of the interlayer is also stabilized, but it is not the global minimum, [and ] there is an energy barrier of  $\sim 1.2kT$  between the midpoint of the interlayer and the  $6.1 \text{ \AA}$  complex.”

Refson *et al.*<sup>S15</sup> obtained an excellent reproduction of Pyrophyllite clay X-Ray structure by energy minimization using DFT method using the Perdew–Wang 91 GGA exchange-correlation functional<sup>S5</sup> and ultrasoft pseudo-potentials.<sup>S9,S10</sup> Pyrophyllite is an anhydrous 2:1 layer type clay belonging to the Pyrophyllite-talc group.<sup>S16</sup> The same clay (Pyrophyllite) was investigated by

Stackhouse *et al.*<sup>S17</sup> to study the hydroxylation-dehydroxylation process by DFT *ab initio* method using the same functionals and pseudopotentials as in Reference S11. Chatterjee *et al.*<sup>S18</sup> used both localized and periodic DFT calculations on a series of monovalent ( $\text{Li}^+$ ,  $\text{Na}^+$ ,  $\text{K}^+$ ,  $\text{Rb}^+$ ,  $\text{Cs}^+$ ) and divalent ( $\text{Mg}^{2+}$ ,  $\text{Ca}^{2+}$ ,  $\text{Sr}^{2+}$ ,  $\text{Ba}^{2+}$ ) cations to monitor their effect on the swelling of clays. They obtained the following activity order for the exchangeable cations:  $\text{Ca}^{2+} > \text{Sr}^{2+} > \text{Mg}^{2+} > \text{Rb}^+ > \text{Ba}^{2+} > \text{Na}^+ > \text{Li}^+ > \text{Cs}^+ > \text{K}^+$ . They showed that, “in case of dioctahedral smectite, the hydroxyl groups play a major role in their interaction with water and other polar molecules in the presence of an interlayer cation.” The software package CASTEP (Cambridge Serial Total Energy Package)<sup>S19</sup> was used for the calculations. CASTEP employs Perdew and Zunger parametrization<sup>S5</sup> of the exchange-correlation energy and Becke–Perdew parametrization<sup>S10</sup> of the exchange-correlation functional. The pseudopotentials were constructed from the CASTEP database and a plane wave basis set for the expansion of the wave functions was used. The screening effect of core electrons was approximated by LDA, while the screening effect for valence electrons was approximated by GGA.

Clausen *et al.*<sup>S20</sup> investigated the adsorption of a number of low-molecular-weight single molecules (including water) on dry sodium smectite clay surface and in a subsequent paper<sup>S21</sup> the adsorption of 2 to 6 water. They used the CPMD software.<sup>S22</sup> For the exchange-correlation functional, the generalized gradient approximation (GGA) was used and, in particular, the Perdew–Burke–Ernzerhof<sup>S23</sup> (PBE) parametrization, which has been demonstrated to describe rather accurately heterogeneous systems, and also the physical properties of water.<sup>S24</sup> Spin-polarization was accounted for in all open-shell systems. Atomic norm-conserving pseudopotentials were derived with the Martins–Trouiller (MT) procedure<sup>S13</sup> and applied using the Kleinman–Bylander scheme<sup>S25</sup> to treat the nonlocal terms. More recently, Liu *et al.*<sup>S26</sup> used CPMD to study the effects of the substitution of Fe on the structure and dynamics of smectite. Finally, Churakov and Kosakowski<sup>S27</sup> performed CPMD simulations to predict the structure and dynamics of hydronium solvation in mono-bi- and trihydrated Na-montmorillonite.

## **Assessing the choice of basis set and other parameters use in CPMD simulations by comparison with accurate *ab initio* calculations for $\text{Na}^+$ - water clusters.**

In order to check the validity of the choices about basis set, DFT functionals and wavefunction cutoff reported in the paper, including the convergence of the CPMD simulations, we performed test calculations for an ensemble of about 300 configurations generated randomly for clusters

containing one ion and one to six water molecules, using CPMD calculations and *ab initio* DFT calculations with the def2-QZVP basis set and the same density functional. The TURBOMOLE package was used for the extended basis set calculations.<sup>S28</sup> The PBE was used in both cases. It can be seen in Figure S1 that the agreement is good.

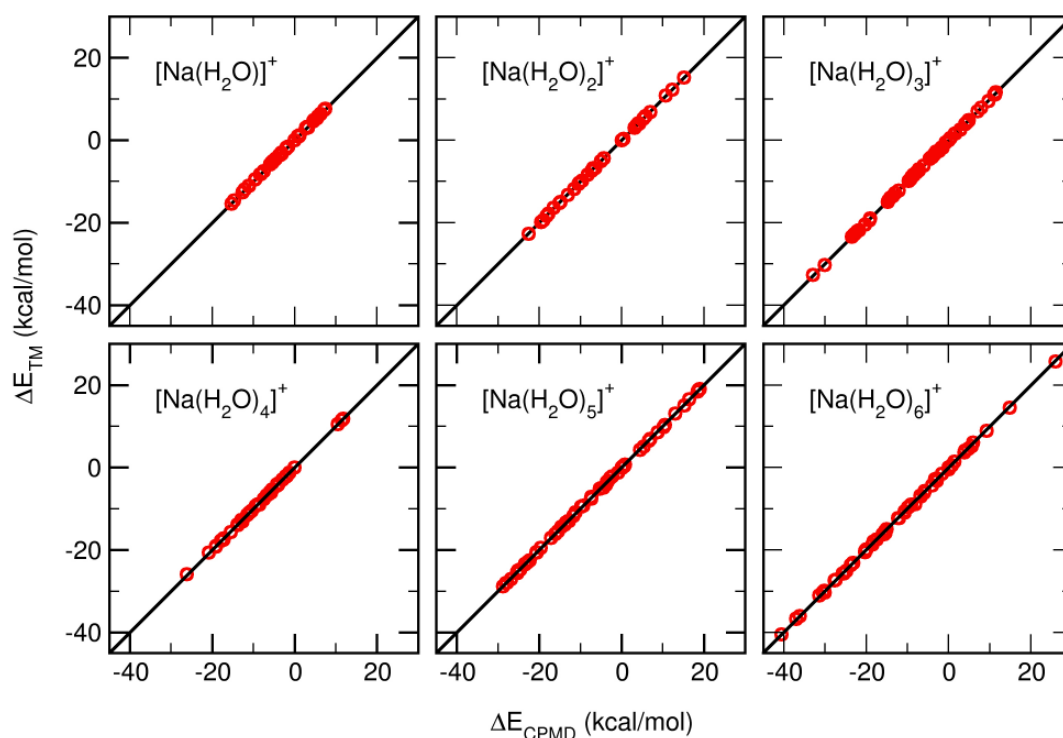


**Figure S1.** Computed binding energy for  $\text{Na}^+(\text{OH})_n$  clusters ( $n = 1$  to  $6$ ) using the CPMD with the basis set and parameters adopted in the current study,  $\Delta E_{\text{CPMD}}$ , vs. *ab initio* DFT calculations with the def2-QZVP basis set using the TURBOMOLE package,<sup>S28</sup>  $\Delta E_{\text{TM}}$ .

## Checking energy conservation and possible deviations from Born-Oppenheimer surface

We checked carefully that the total energy is well conserved and that the CPMD energy surface is parallel to the Born-Oppenheimer one. In the top panel of Figure S2 we show the energy conservation during almost 50 ps of NVE simulation. It can be seen that there is no drift in the conserved quantity of the extended Lagrangian system. In addition, the Kohn-Sham energy fluctuates around a constant value and it does not show any abnormal behaviour. The blue box

highlights the region which has been blown-up in the bottom left panel. There, the Car-Parrinello (CP) energy over a short time interval is compared with the Born-Oppenheimer (BO) energy for twenty randomly chosen configurations. The energy threshold for the SCF convergence in the BO calculation was chosen to be  $10^{-7}$  a.u. It can be seen that the CP trajectory closely follows the BO surface, being it only slightly offset. To better appreciate the agreement between data, in the bottom right panel we show the correlation plot between the two energies for the twenty configurations chosen. Since the energy does not show any appreciable drift over the time span of the simulations, and given that the CP and BO energies agree even at long times, we are confident about the validity of our electronic structure calculations.

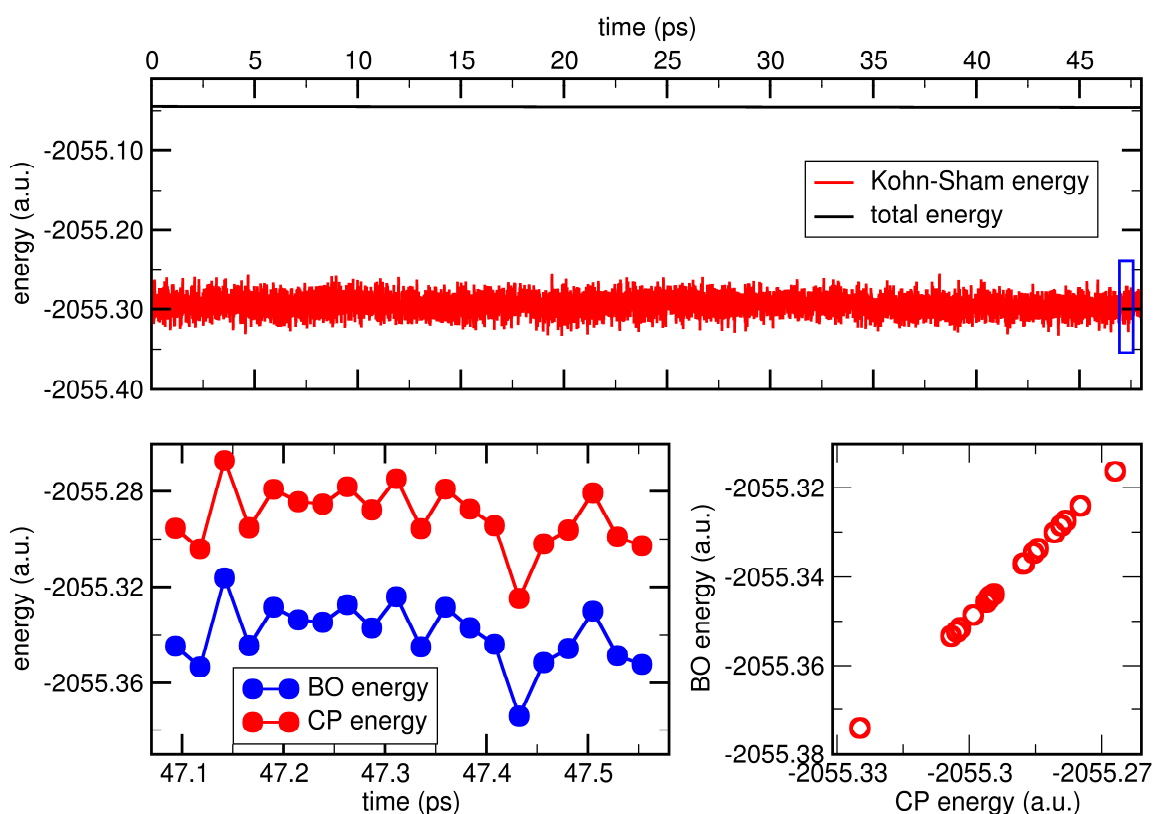


**Figure S2.** Top: Total and Kohn-Sham energies during almost 50 ps of NVE simulation. The blue box highlights the region which has been blown-up in the bottom left panel. Bottom left: Car-Parrinello (CP) energy over a short time interval compared with the Born-Oppenheimer (BO) energy. Bottom right: correlation plot between the two energies for the twenty configurations chosen.

## Evaluation of crystallographic coordinates, distances and angles and of vibrational spectra.

Initially, the atomic positions were generated by applying space group symmetry transformations to the crystallographic atomic coordinates of the asymmetric unit. The average coordinates of a given atom of the asymmetric unit were evaluated using the cumulative distributions of each coordinate obtained by back-transforming the current crystallographic positions of all the atoms symmetry related to the same asymmetric unit atom and adding them to the distributions. Narrow Gaussian-like cumulative distributions are the results of an optimal reproduction of the crystal symmetry, whereas multimodal distributions indicate that the symmetry is not maintained, and asymmetric or unexpectedly large ones are the sign of static or dynamic disorder.<sup>S29</sup>

A similar procedure was used to evaluate intramolecular bond distances and angles. Instead of the naïve values derived by using average atomic positions, the distributions of these quantities were computed from the instantaneous atomic coordinates, and the averages were computed as the first moments of these distributions.<sup>S29</sup> This procedure allows to take into account anharmonic oscillations and other anomalies, which also can be evidenced by the shape of the distributions themselves. Some information is deserved about Reference S29, as is not available online. It was about the classical molecular dynamics simulation of Natrolite, a natural zeolite containing sodium cations and one water molecule per cation. A flexible water model was adopted, and the above procedures were proposed and used to evaluate crystallographic coordinates, bond distances and angles.

Vibrational spectra were derived from Fourier transforms of the velocity autocorrelation function (VACF) of the atomic nuclei, but using a sophisticated procedure proposed by Berens *et al.*<sup>S30</sup> In order to avoid spurious effects caused by the finite-time trajectories generated by MD simulations, before evaluating the Fourier transform the VACF is multiplied by a function which approaches to zero close to the initial and final time of the simulation but does not affect substantially its value far from the extreme times. This procedure is called windowing. Many different windowing functions were discussed by Harris<sup>S31</sup> and, as proposed by Berens *et al.*,<sup>S30</sup> we used the Blackmann-Harris windowing function. The resulting spectra, however, due to an incomplete sampling of all possible oscillation frequencies, appear noisy, with many close meaningless peaks, which make the interpretation and the comparison with the experiments difficult. This problem was overcome by Nicholas *et al.*,<sup>S32</sup> who proposed to smooth the computed spectra by the side averaging procedure. In addition, this procedure permits to evaluate the

vibrational properties of selected groups of atoms separately, such as the aluminosilicate sheets, the cations or the water molecules.

### **The evaluation of errors of structural data in X-ray experimental reports.**

It is well-known that in single-crystal X-ray or neutron diffraction structure determination, the atomic coordinates are derived by a fitting procedure, aiming at minimizing the deviations between the absolute values of the observed and calculated scattering amplitudes.<sup>S33-36</sup> The final value of the sum of these deviations divided by the sum of the experimental amplitudes is called R-factor. Structure determinations with R-factor less than 0.1 are considered as “good” (in Reference 15 and 16 the average R-factors are 0.12 and 0.128, respectively), but there is no general criteria for assessing the standard error of the single coordinates. The computed scattering amplitudes include the Debye-Waller (DW) factor, containing the mean square displacement of the atoms, which can be isotropic (a scalar) or anisotropic (a symmetric tensor of rank 3, with six independent elements). As ascertained by theoretical calculations and by accurate crystal structures, at room temperature the reasonable values of DW factors in minerals should correspond to a mean linear displacement at most of the order of a few tenths of Å. Therefore, if an atomic DW factor largely exceeds this estimate, probably some disorder affects the position of that atom, some error was made in the choice of symmetry group or, sometimes, the number and the quality of the recorded reflections is not sufficient.

Nevertheless, the most common use is to report the final values of the atomic fractional or crystallographic coordinates (assuming as units the crystallographic unit cell sides, therefore falling in the range from -1 to 1) with four digits, assuming that the fifth one is uncertain. If a coordinate corresponds to a symmetry element (e.g., a mirror plane) the error is zero in crystallographic units, but in length units it depends on the error of the cell parameters, which sometimes is given as standard error. As often the unit cell axes are substantially different, also this uncertainty, in length unit, is different.

The problem is made even more involved because the X-ray diffraction yield the electronic density of the crystal, from which the position of the nuclei is inferred by supposing that the distribution is spatially symmetric with respect to the nuclei, whereas neutron diffraction is sensitive to the positions of the nuclei themselves.<sup>S36</sup> In both cases errors can be caused by asymmetric thermal motion, twinning of the crystals, chemical or isotopic defects, and many others. Therefore, the actual error of the atomic coordinates in units of length must be ascertained by some empirical “external” criteria as the comparison between structures similar compounds or between the

structures of the same crystal obtained by both diffraction methods and/or at different temperature, preferably very low (assuming no phase transition), and when available, with an R-factor very small (3-5%).

In practice, excluding the crystals where all the atom are in special positions, which are not at all frequent, and by considering the average anharmonicity of thermal oscillation amplitudes, the actual physical error of the experimental coordinates is estimated at best of the order of 0.005-0.01 Å. As cell sides, for minerals, range from a few Ångstroms to a few tens of Ångstroms, the fifth digit corresponds to an error of the order of  $10^{-4}$ - $10^{-3}$  Å, or to the smallest reasonably possible value. Sometimes, especially if a given coordinate of an atom entails an anomalous bond distance or that atom shows an exceedingly large DW factor, indicating some static or dynamic disorder, its value is given by using three or two digits or by reporting an “uncertainty” such as: 0.1234(15), meaning  $0.1234 \pm 0.0015$ , but this “uncertainty” is not to be intended exactly as a standard error. Therefore, in Table 1 we compare only *average* values, which are the “exact” result of a well-defined calculation and in Table 2 experimental average values are reported.

Bond distances and angles are usually evaluated by using the average atomic coordinates, thus implying that the motion of all nuclei is symmetric about the average position and completely uncorrelated. If the details of the motion were known, the averages could include anharmonicity and correlation effects, but the “true” dynamics in crystals is essentially quantum mechanical, because of the presence of zero-point oscillations and the averages should include also this effect, which is negligible only in case of perfectly symmetric motion. In our simulations, the motion of the nuclei follows the classical mechanics, but error sources can be partially avoided by using the above reported averaging procedure using the distributions of the variables.

## **Distribution functions.**

We report some details of the results which were omitted in the paper. In Figure S3 the computed  $\text{Na}^+ - \text{H}_w$  (water hydrogens) radial distribution function (RDF) is plotted. The maximum at 2.89 Å, indicates that hydrogen atoms point mainly out of the cation, as expected, because the maximum of the  $\text{Na}^+ - \text{O}_w$  (Figure 4) falls at 2.89 Å. The vertical scale is omitted because RDFs bear incomplete information for adsorbed species as discussed in Reference S37. This remark holds also for Figure S5.

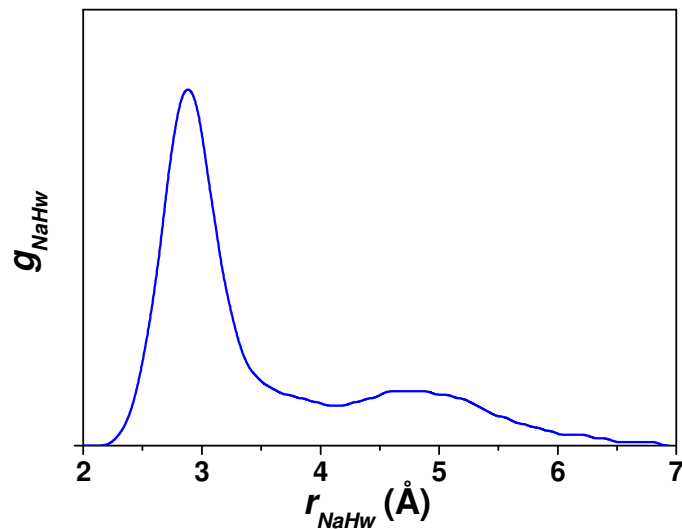


**Figure S3.** Computed  $\text{Na}^+ - \text{H}_w$  radial distribution function (RDF).

Figure S4 shows the time evolution of the coordination number of water around the  $\text{Na}^+$  cations  $n(\text{Na})$  for each cation separately. To evaluate  $n(\text{Na})$ , the instantaneous number of  $\text{O}_w$ s with  $\text{Na}^+ - \text{O}_w < 3.2 \text{ \AA}$ , the distance corresponding to the first minimum of  $\text{Na}^+ - \text{O}_w$  RDF. The vertical scales are shifted to make the plot more legible. In Figure S4 the computed  $\text{O}_s$  (silicate sheet oxygens) –  $\text{O}_w$  RDF is reported. The maximum falls at  $2.72 \text{ \AA}$ , a value similar to that in bulk water, while for the  $\text{O}_s - \text{H}_w$  RDF it falls at  $1.72 \text{ \AA}$ , what is typical of a HB between adsorbed water and the basal oxygens of the sheet.

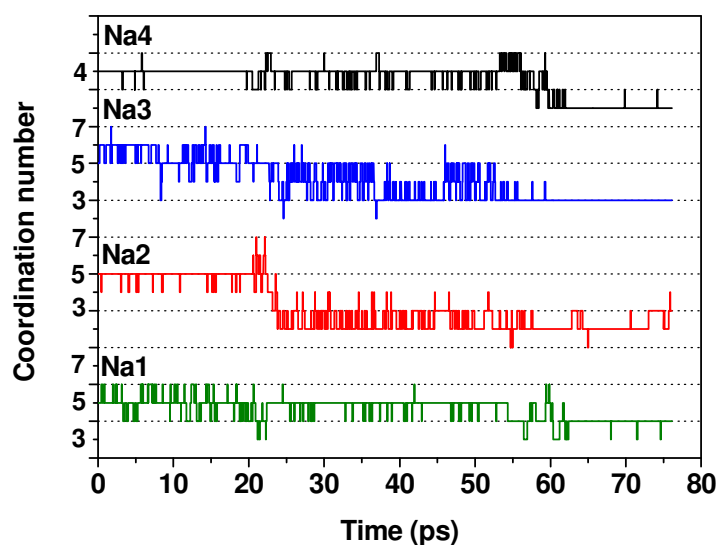


**Figure S4.** Time evolution of coordination number for each  $\text{Na}^+$  cation.

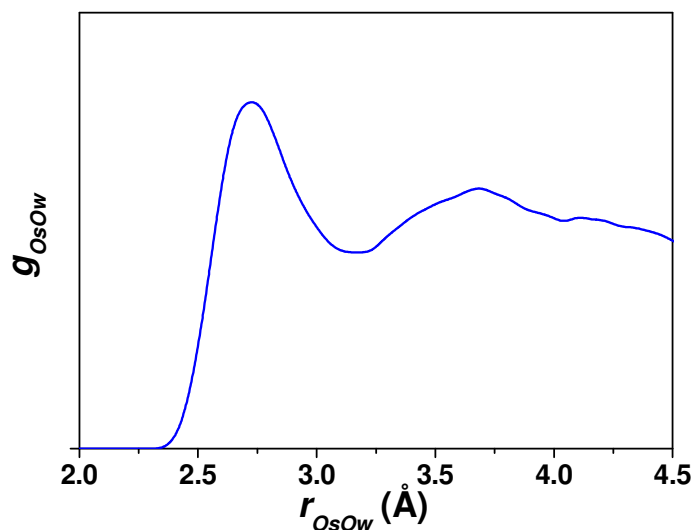


**Figure S5.** Computed O<sub>S</sub> (silicate sheet oxygens) – O<sub>w</sub> RDF.

## References

- (S1) Boulet, B.; Greenwell, H. C.; Stackhouse, S.; Coveney, P. V. *J. Mol. Struct. THEOCHEM* **2006**, 762, 33-48.
- (S2) Tunega, D.; Benco, L.; Haberhauser, G.; Gerzabek, M. H., Lischka, H. *J. Phys. Chem. B* **2002**,
- (S3) Sposito, G. *The Chemistry of Soils*, Oxford Univ. Press: New York, 1989.
- (S4) Sposito, G. *The Surface Chemistry of Soils*, Oxford Univ. Press: New York, 1984.
- (S5) Perdew, J. P.; Zunger, A. *Phys. Rev. B* **1981**, 23, 548.
- (S6) Perdew, J. P.; Wang, Y. *Phys. Rev. B* **1992**, 45, 13244–13249.
- (S7) Blöchl, P. E.; Parrinello, M. *Phys. Rev. B* **1992**, 45, 9413.
- (S8) Kresse, G.; Joubert, D. *Phys. Rev. B* **1999**, 59, 1758.
- (S9) Vanderbilt, D. *Phys. Rev. B* **1990**, 41, 7892.
- (S10) Becke, A. D. *Phys. Rev. A* **1988**, 38, 3098–3100.
- (S11) Boek, E. S.; Sprik, M. *J. Phys. Chem. B* **2003**, 107, 3251-3256.
- (S12) Lee, C.; Yang, W.; Parr, R. G. *Phys. Rev. B* **1988**, 37, 785–789.
- (S13) Troullier, N.; Martins, J. L. *Phys. Rev. B* **1991**, 43, 1993-2006.
- (S14) Suter, J. L.; Boek, E. S.; Sprik, M. *J. Phys. Chem. C* **2008**, 112, 18832-18839.
- (S15) Refson, K.; Park, S.-H.; Sposito, G. *J. Phys. Chem. B* **2003**, 107, 13376-13383.
- (S16) Wardle, R.; Brindley, G. W., *Am. Mineral.* **1972**, 57, 732-750.
- (S17) Stackhouse, S.; Coveney, P. V.; Benoit, D. M. *J. Phys. Chem. B* **2004**, 108, 9685-9694.
- (S18) Chatterjee, A.; Ebina, T.; Onodera, Y.; Mizukami, F. *J. Chem. Phys.* **2004**, 120, 3414-3424.

- (S19) Payne, M. C.; Teter, M. P.; Allan, D. C.; Arias, T. A.; Johannopoulos, J. D. *Rev Mod. Phys.* **1992**, *64*, 1045-1097.
- (S20) Clausen, P.; Andreoni, W.; Curioni A.; Hughes, E; Plummer, C. J. G. *J. Phys. Chem. C*, **2009**, *113*, 12293-12300.
- (S21) Clausen, P.; Andreoni, W.; Curioni A.; Hughes, E; Plummer, C. J. G. *J. Phys. Chem. C*, **2009**, *113*, 15218-15225.
- (S22) CPMD Copyright IBM Corp 1990–2008; Copyright MPI für Festkörperforschung Stuttgart 1997–2001; see [www.cpmc.org](http://www.cpmc.org).
- (S23) Perdew, J. P.; Burke, K.; Ernzerhof, M. *Phys. Rev. Lett.* **1996**, *77*, 3865-3868
- (S24) Grossman, J. C.; Schwegler, E.; Draeger, E. W.; Gygi, F.; Galli, G. *J. Chem. Phys.* **2004**, *120*, 300-311.
- (S25) Kleinman, L.; Bylander, D. M. *Phys. Rev. Lett.* **1982**, *48*, 1425-1428.
- (S26) Liu, X.; Meijer, E. J.; Lu, X.; Wang, R. *Clays and Clay Miner.* **2010**, *58*, 89-96.
- (S27) Churakov, S. V.; Kosakowski, G. *Philos. Magaz.* **2010**, *90*, 2459-2474.
- (S28) TURBOMOLE V6.4 2012, a development of University of Karlsruhe and Forschungszentrum Karlsruhe GmbH, 1989-2007, TURBOMOLE GmbH, since 2007; available from: <http://www.turbomole.com>
- (S29) Demontis, P.; Suffritti, G. B.; Alberti, A.; Quartieri, S.; Fois, E. S.; Gamba, A., *Gazz. Chim. Ital.*, **1986**, *116*, 459-466
- (S30) Berens, P.H.; White, S. R.; Wilson, K.R. *J. Chem. Phys.* **1981**, *75*, 515-529.
- (S31) Harris, F. H. *Proc. IEEE* **1978**, *66*, 51-83.
- (S32) Nicholas, J.B.; Hopfinger, A. J.; Trow, F. R.; Iton, L. E. *J. Am. Chem. Soc.* **1991**, *113*, 4792-4800.
- (S33) *Fundamentals of Crystallography*: Giacovazzo, C., Ed.; International Union of Crystallography Book Series, No. 2, Oxford Univ. Press: Oxford, 2011.
- (S34) Stout, G. H.; Jensen, L. H. *X-Ray Structure Determination: A Practical Guide, 2nd Edition*, John Wiley and Sons, New York, 1989.
- (S35) Moore, D. M.; Reynolds, R. C. *X-Ray Diffraction and Identification and Analysis of Clay Minerals*, Oxford Univ. Press: New York, 1997.
- (S36) Willis, B. T. M.; Carlile, C. J. *Experimental Neutron Scattering*, Oxford University Press: Oxford, 2009.
- (S37) Demontis, P.; Gulín González, J.; Suffritti, G. B. *J. Phys. Chem. C* **2012**, *116*, 11100–11109.